Insights into Electrophysiological Studies with Papillary Muscle by Computational Models

Frank B. Sachse[1], Gunnar Seemann[2], and Bruno Taccardi[1]

[1]Nora Eccles Harrison Cardiovascular Research and Training Institute,
University of Utah, UT, USA
fs@cvrti.utah.edu
http://www.cvrti.utah.edu
[2]Institut für Biomedizinische Technik,
Universität Karlsruhe (TH), Germany
http://www-ibt.etec.uni-karlsruhe.de

Abstract. Basic electrical properties and electrophysiological mechanisms of cardiac tissue have been frequently researched applying preparations of papillary muscle. Advantages of these preparations are the simplicity to satisfy their metabolic demands and the geometrical elementariness in comparison to wedge and whole heart preparations. In this computational study the spatio-temporal evolution of activation fronts in papillary muscle was reconstructed with a bidomain model of electrical current flow and a realistic electrophysiological model of cardiac myocytes. The effects of two different pacing sites were investigated concerning the distribution of extracellular potentials and transmembrane voltages. Results of simulations showed significant changes of the resulting wave fronts and the related potential distributions inside of the muscle and in the bath for the different pacing sites. Additionally, the results indicated that reliable measurements of activation times can be carried out only in regions adjacent to the wave front. These results can be applied for development of measurement setups and techniques for analysis of experimental studies of papillary muscle.

1 Introduction

Papillary muscles have been frequently applied in experimental studies to characterize electrical properties of myocardium and spread of electrical excitation under varying conditions [1–6]. In attempts to reconstruct measurement data and to support analysis of these data, the electrophysiological properties of papillary muscles were studied also with several computational models [7–11],

This computational study aims at guiding future development of measurement setups and techniques for analysis of electrophysiological experiments with papillary muscles. Particularly, this study parallels an experimental study of mechano-electrical feedback mechanisms in excised papillary muscle from rabbits [5]. A crucial component of the analysis in this and other experimental

A.F. Frangi et al. (Eds.): FIMH 2005, LNCS 3504, pp. 216–225, 2005.

studies is the accurate detection of activation times from analysis of bath voltage measurements near to the surface of the muscle.

Extraction of local activation times was applied e.g. to create activation and isochrone maps as well as to determine conduction velocity. While detection of activation times in transmembrane voltage recordings is possible with simple numerical methods, detection in electrograms in the bath is challenging due to interferences from non-related electrical sources and a commonly significantly smaller signal-to-noise ratio. Further complexity is added by geometrical relationships between the positions of the measurement electrodes, the activation front and its spatial domain.

The computational study had two specific aims: (1) The spatio-temporal evolution of activation fronts and the related extracellular and bath voltage distributions were determined and analyzed for two different stimulus electrode arrangements. (2) The relationship between activation times detected in the bath and from the transmembrane voltage in the muscle, respectively, was investigated.

The computational study was carried out with an anisotropic bidomain model of papillary muscle in a bath. The model was created using simplified geometrical descriptions and applied in numerical experiments. The experiments were designed to reproduce experimental conditions, where a stimulus was given at one end of the preparation and electrograms are acquired at some points along its surface.

2 Methods

2.1 Experimental Conditions

In previous work we developed a software-controlled experimental setup for studying cardiac mechano-electrical feedback of excised papillary muscle in a physiological environment [5]. The setup allows measurement of intracellular and bath electrograms as well as tension of the muscle under various strain conditions. During the measurements the muscle was placed in a horizontal flow-through chamber filled with a modified Tyrode solution of temperature of 37^oC.

The measurement procedure was automated and necessitates only minor user interaction. Electrical signals were acquired from a set of positions, which were determined from a set of points given by the user through steering a pointer with the motorized manipulator. The coordinates of these points were read digitally from a motorized micro-manipulator. Commonly, the recording electrode served as pointer and points at the ends of the muscle were selected. The given coordinates were applied to describe line segments or quadrangles, which were discretized to define measurement positions using sampling of finite element shape functions [12].

2.2 Computational Model

A computational model was created to mirror relevant aspects of the previously described experimental setup. Central component of the model was an bidomain

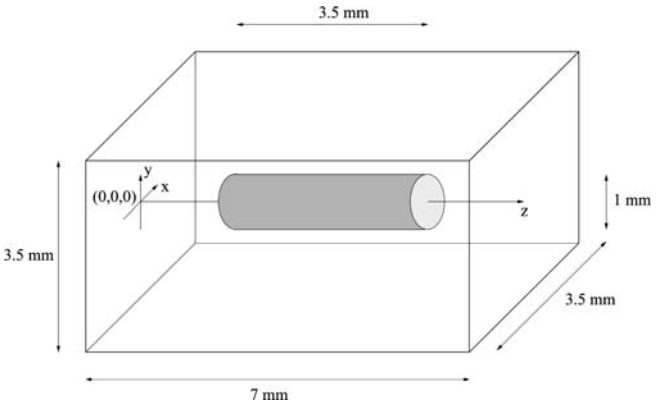

Fig. 1. Model of papillary muscle in bath. The muscle is represented by a cylinder, which is centered in the bath.

description used to reconstruct excitation propagation as well as the corresponding intra- and extracellular as well as bath potential distribution [13].

The bidomain model was based on a simplified geometrical description of the papillary muscle, the bath, and the reference electrode. The model included anisotropic intra- and extracellular conductivities as well as a biophysically detailed cellular electrophysiological model, i.e. the Noble-Kohl-Varghese-Noble model of a ventricular myocyte from guinea-pig [14]. For both domains the generalized Poisson's equation for electrical current fields was applied, which was discretized with the finite element method on hexahedral grids consisting of 70 x 70 x 140 elements in x-, y-, and z-direction (fig. 1). Each element was cubic with an edge length of 50 μm. A cylinder with a diameter of 1 mm and a length of 3.5 mm was rendered in the grids associated to the two domains to represent the papillary muscle. The long axis of the cylinder and the fiber orientation were chosen to be parallel to the z-axis. In summary, 24779 voxels were assigned to papillary muscle, 661221 voxels to bath.

Node variables were associated with the vertices of the hexahedrons [12]. In the finite element approach used in this work a trilinear polynomial was applied to interpolate intra-, extracellular and bath potentials as well as transmembrane voltages and conductivities inside of the hexahedrons. Integration of energy in the elements was carried out with 8-point Gaussian quadrature. A modification of this quadrature technique allowed to respect non-flow conditions at the boundary of the muscle's intracellular space.

The following conductivities were chosen (in S/m) [18]: myocardium extracellular longitudinal $\sigma_{e,l} = 0.375$ and transversal $\sigma_{e,t} = 0.214$, myocardium intracellular longitudinal $\sigma_{i,l} = 0.375$ and transversal $\sigma_{i,t} = 0.0375$, and bath $\sigma_b = 1.5$.

The Euler forward method with a temporal resolution of 10 μs was used to solve the ordinary differential equations associated with the electrophysiological model [15]. At each time step the Poisson equation attributed to the extracellular

space and bath was solved with an over-relaxation method. An over-relaxation factor $\lambda = 1.85$ was chosen.

Two different pacing sites were chosen: central and superficial at the left end of the muscle. A stimulus current was applied extracellularly at $t = 0\ ms$ for a duration of 1 ms at the center and a peripheral position, respectively, of the left circular face of the cylinder. The magnitude of the stimulus current was chosen in such a manner that a propagating front was initiated. Additionally, Dirichlet boundary conditions were defined on the right side of the bath, i.e. the extracellular potential at position (0,0,7) mm was set to zero.

Parallelization of computationally expensive tasks was achieved on basis of the OpenMP API [16]. The simulations were performed on a Silicon Graphics Origin 3000 compute server with 32 GB of main memory and 64 processors of type R14000/600 MHz. In both simulations 24 processors were employed, each for $\approx$ 40 h.

2.3 Detection of Activation Time

In this work the activation time in computed courses of transmembrane voltages and bath electrograms was detected by searching for the maximal and minimal temporal derivative, respectively [17, 18]. The search was restricted to a time window after the stimulus.

3 Results

The spread of excitation through the papillary muscle was simulated for central and superficial stimulation (figs. 2 and 4). The simulation was carried out for a time interval starting from stimulation to full excitation of the preparation.

Central Stimulation. In initial phases of the simulation a high curvature of the propagation front was found reflecting the anisotropy of conductivities (fig. 2, 2ms). This phase was followed by a decrease of curvature. In the last phase of spread, when the front reached the right end, a small curvature was found (fig. 2, 12ms).

Superficial Stimulation. The simulation showed activation fronts shaped significantly by the anisotropic properties of myocardium (fig. 4). The conduction velocity vector was composed of a large longitudinal and small transverse components. Full excitation of the preparation was found 2 ms earlier than for central stimulation.

In both simulations, transmembrane voltages ranged between -92 and 48 mV as well as extracellular and bath potentials were between -25 and 10 mV. Both, the transmembrane voltages and extracellular potentials showed largest magnitudes of their spatial gradients at the propagation front (figs. 3 and 5). Isolines of extracellular potentials and transmembrane voltage were partly of similar shape inside of the muscle.

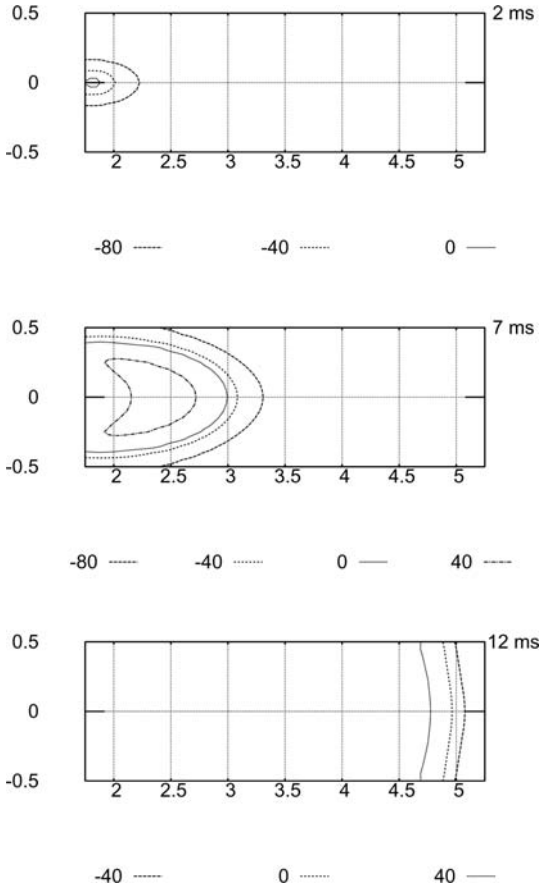

Fig. 2. Transmembrane voltages in XZ-slice through the long axis of muscle. The excitation was initiated with an electrical stimulus in the extracellular space at the center of the left border of the muscle, i.e. position (0, 0, 1.75). The three panels show isolines of voltages at 2, 7, and 12 ms. The style of the isolines codes voltages in mV. The scaling of the axes is in mm

Activation times at different positions were detected from the extracellular potentials and transmembrane voltages (fig. 6). The activation times detected in transmembrane voltages for central and superficial stimulation indicated differences of related activation fronts and boundary effects. A significant initial offset of ≈ 4.3 ms was found (fig. 6a), which was followed be a decrease due to the higher velocities for superficial stimulation. In the final phase of propagation, the activation time offset averaged to ≈ 2 ms. Reliable detection of activation times in extracellular electrograms was partly not possible due to their small slopes (fig. 6b,c). A non-constant offset between the activation time courses was observed. In general, the relationship between activation time and distance was found to be nonlinear particularly at the left and right end of the preparations.

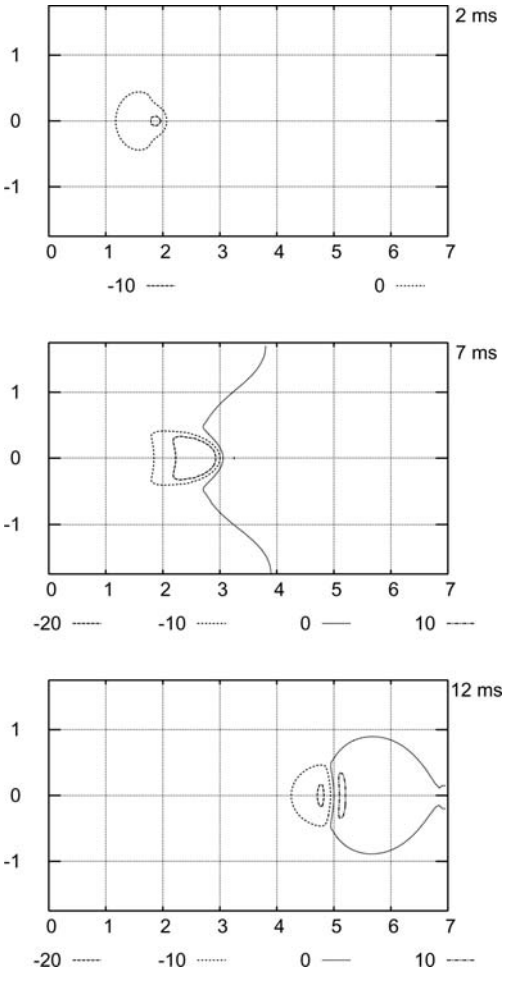

Fig. 3. Extracellular and bath potentials corresponding to fig. 2

4 Conclusions

The study revealed that excitation propagation in papillary muscle is a three-dimensional process, which can only poorly be described by uni-dimensional approximations. The simulations showed significant differences of the spatio-temporal evolution of activation fronts and related potential distributions resulting from central and superficial stimulation.

Already in the case of central stimulation, the curvature of the wave front, particularly near the stimulus site, led to radial differences of the transmembrane voltage and related detected activation times. These radial heterogeneities of transmembrane voltage led to radial heterogeneities of electrical fields in the bath and differences of therein detected activation times. Additional hetero-

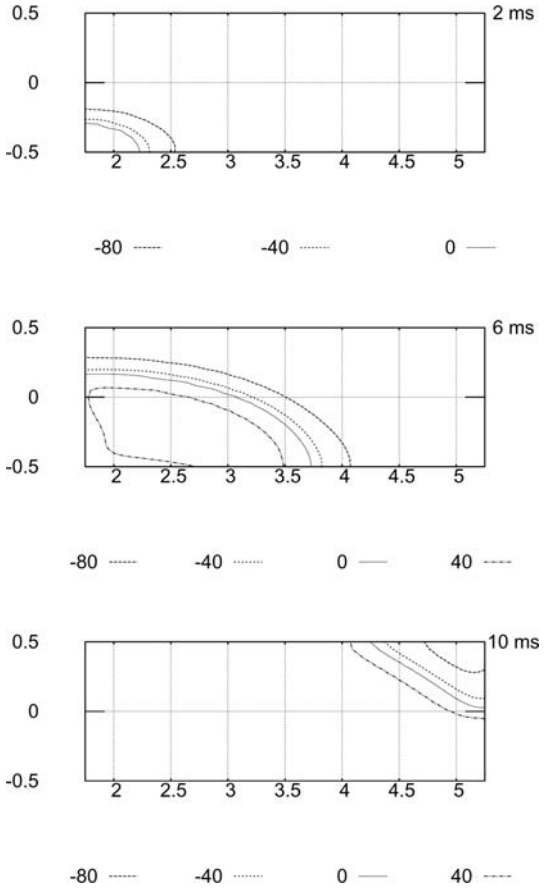

Fig. 4. Transmembrane voltages in XZ-slice through the long axis of muscle. The excitation was initiated with an electrical stimulus in the extracellular space at the lower left border of the muscle, i.e. position (-0.5, 0, 1.75)

geneities with a significant non-radial component were found for the superficial stimulation. Thus, particularly at the ends of the preparation the linearity of the relationship of activation time and distance degrades significantly as the distance of measurement position to the preparation increases. These findings confirms that conduction velocity can be detected with a given accuracy only in specific areas, which are defined by their neighborhood to the activation front.

For both cases of stimulation, the wave front was initially convex and afterwards its curvature decreased. In case of superficial stimulation the wave front was concave during the final phase of simulation (fig. 4 10ms). Other studies reported a steady state of conduction velocity associated with a concave curvature for a cylindrical strand of cardiac muscle [17, 18]. A steady state was not reached in our study, which can be explained by the relatively short length of our preparation, i.e. 3.5 versus 12.8 mm. Additionally, the type and location of

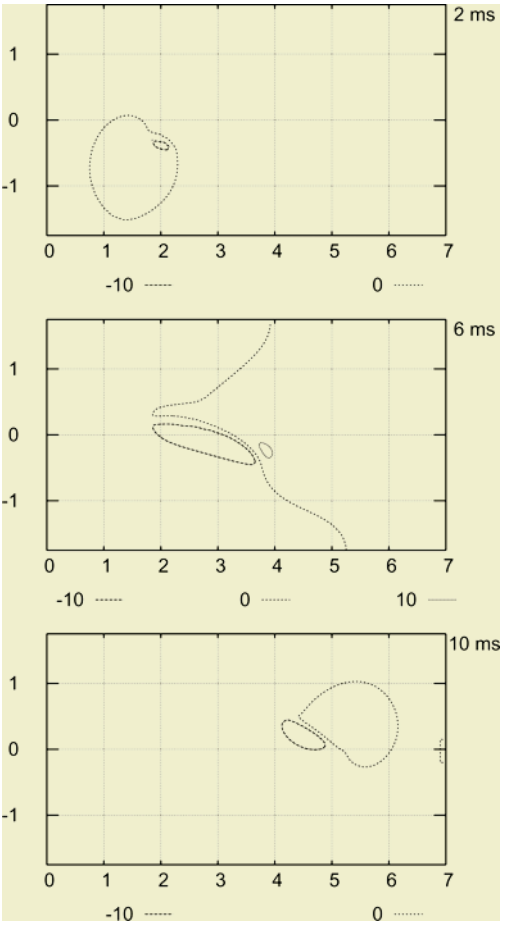

Fig. 5. Extracellular and bath potentials corresponding to fig. 4

stimulus electrodes applied in our study, i.e. central and superficial point versus ring electrodes, will increase the time until steady state is reached.

Future work will necessitate research concerning more efficient numerical methods to solve the bidomain model. Particularly, we are interested to reduce the high computational demand associated with solution of Poisson's equation associated to the extracellular space, e.g. by applying mesh-less techniques for solving of differential equations, and the high temporal resolution necessary to solve ordinary differential equations with the Euler method.

Acknowledgments

This work has been supported by the Richard A. and Nora Eccles Fund for Cardiovascular Research and awards from the Nora Eccles Treadwell Foundation.

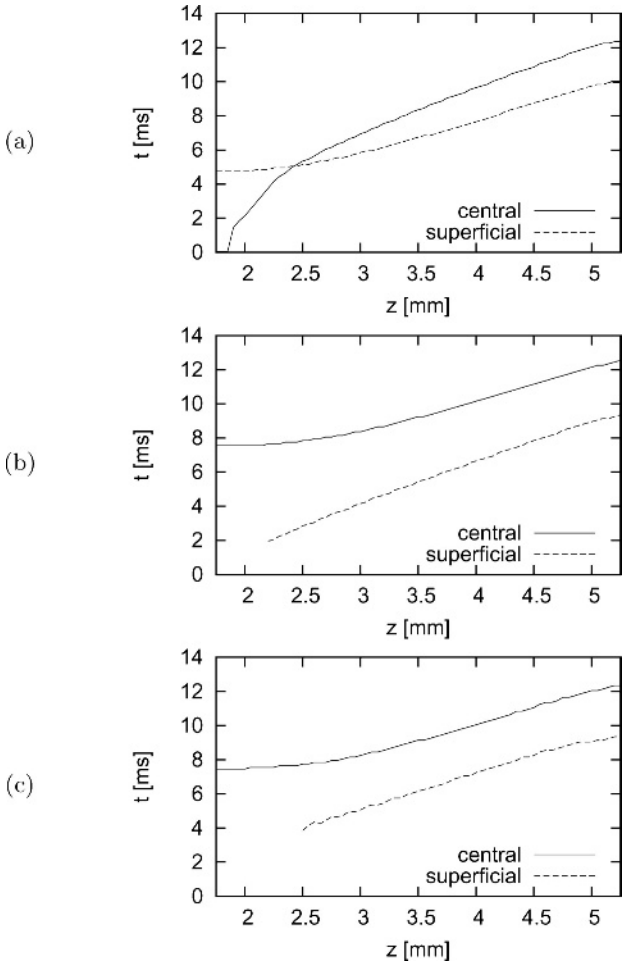

Fig. 6. Activation times detected for central and superficial stimulation. (a) The time of maximal derivative delivered activation from the transmembrane voltage at (0,0,z). The time of minimal derivative of the extracellular potentials in the bath at a distance of (b) 25 μm and (c) 275 μm to muscle surface determined activation

The authors gratefully acknowledge computing resources kindly provided by the Scientific Computing and Imaging Institute and the NIH NCRR Center for Bioelectric Field Modeling, Simulation, and Visualization.

References

1. Fleischhauer, J., Lehmann, L., Kléber, A.G.: Electrical resistances of interstitial and microvascular space a determinants of the extracellular electrical field and velocity of propagation in ventricular myocardium. Circ. **92** (1995) 587–594

2. Kléber, A.G., Riegger, C.B.: Electrical constants of arterially perfused rabbit papillary muscle. J. Physiol. **385** (1987) 307–324
3. Penefsky, Z.J., Hoffman, B.F.: Effects of stretch on mechanical and electrical properties of cardiac muscle. Am. J. Physiol. **204** (1963) 433–438
4. Saeki, Y., Kurihara, S., Komukai, K., Ishikawa, T., Takigiku, K.: Dynamic relations among length, tension, and intracellular Ca^{2+} in activated ferret papillary muscles. Am. J. Physiol. **275** (1998) H1957–H1962
5. Sachse, F.B., Steadman, B.W., Bridge, J.H.B., Punske, B.B., Taccardi, B.: Conduction velocity in myocardium modulated by strain: Measurement instrumentation and initial results. In: Proc. 26th Conf. IEEE EMBS. (2004)
6. Spear, J.F., Moore, E.N.: Stretch-induced excitation and conduction disturbances in the isolated rat myocardium. J. Electrocardiology **5** (1972) 15–24
7. Henriquez, C.S., Plonsey, R.: A bidomain model for simulating propagation in multicellular cardiac tissue. In: Proc. of the Annual International Conference of the IEEE Engineering in Medicine and Biology Society. Volume 4. (1989) 1266
8. Henriquez, C.S., Plonsey, R.: Simulation of propagation along a cylindrical bundle of cardiac tissue–II: Results of simultions. IEEE Transactions on Biomedical Engineering **37** (1990) 861–875
9. Henriquez, C.S.: Simulating the electrical behaviour of cardiac tissue using the bidomain model. Critical Reviews in Biomedical Engineering **21** (1993) 1–77
10. Roth, B.J.: Action potential propagation in a thick strand of cardiac muscle. Circ. Res. **68** (1991) 162–173
11. Sachse, F.B., Seemann, G., Weiß, D.L., Punske, B., Taccardi, B.: Accuracy of activation times detected in simulated extracellular electrograms. In: Proc. Computers in Cardiology. (2004)
12. Schwarz, H.R.: Methode der finiten Elemente. 3 edn. Teubner, Stuttgart (1991)
13. Sachse, F.B.: Computational Cardiology: Modeling of Anatomy, Electrophysiology, and Mechanics. LNCS 2966. Springer, Berlin, Heidelberg, New York (2004)
14. Noble, D., Varghese, A., Kohl, P., Noble, P.: Improved guinea-pig ventricular cell model incorporating a diadic space, I_{Kr} and I_{Ks}, and length- and tension-dependend processes. Can. J. Cardiol. **14** (1998) 123–134
15. Press, W.H., Teukolsky, S.A., Vetterling, W.T., Flannery, B.P.: Numerical Recipes in C. 2 edn. Cambridge University Press, Cambridge, New York, Melbourne (1992)
16. Open Architecture Review Board: OpenMP: Simple, portable, scalable SMP programming (1997-2004)
17. Spach, M.S., Barr, R.C., Serwer, G.A., Kootsey, J.M., Johnson, E.A.: Extracellular potentials related to intracellular action potentials in the dog purkinje system. Circ. Res. **30** (1972) 505–519
18. Punske, B.B., Ni, Q., Lux, R.L., MacLeod, R.S., Ershler, P.R., Dustman, T.J., Allison, M.J., Taccardi, B.: Spatial methods of epicardial activation time determination in normal hearts. Annals Biomed. Eng. **31** (2003) 781–792